ID-1194

FABRICATION AND MECHANICAL PROPERTIES OF SINTERED SiC FIBER REINFORCED SiO_2-MULLITE COMPOSITES

K. Nagahisa[1], K. Kitatani[1], K. Iwamoto[1], M. Yoshida[2], G. Sasaki[2] and H. Fukunaga[2]
[1]*Graduate school of Hiroshima university*
[2] *Department of Mechanical Engineering, Hiroshima University, Kagamiyama 1-4-1, Higashi-Hiroshima, 739- 8527, Japan*

SUMMARY: A sintered SiC fiber reinforced SiO_2-mullite composites were fabricated by impregnation of the fiber tows into matrices slurry and hot pressing.

In order to control the nature of residual stress in the composites, the matrix of three levels of Al_2O_3 content in SiO_2- mullite were prepared. Tyranno SA fiber was selected for the reinforcement because of high-temperature phase stability. The obtained composites had well dense structure, and both mullite and glassy SiO_2 phases were found in the matrices. Volume fraction and morphology of the mullite were dependent on the extent of super saturation of Al_2O_3 in the under cooled liquid. Interfacial chemical reaction between fiber and oxide matrix due to fabrication process was not observed. The nature of thermal residual stress in the composites was controlled by Al_2O_3 content in SiO_2-mullite hypereutectic oxide material, which was analyzes by finite element method (FEM) and by measuring interfacial shear stress with fiber push-out test.

Three-point flexural strength of the composites at room temperature were 1254 MPa (3.7 mol.% Al_2O_3) and 967 MPa (30 mol.% Al_2O_3). Fracture behavior was non-catastrophic with fiber-pull out in the fracture surface. The highest flexural strength of the SiO_2-3.7 mol.% Al_2O_3 matrix composite will be caused by the highest compressive residual stress in the matrix.

KEYWORDS: CFCC, Residual stress, SiC fiber, Oxide matrix, Solidification, Mechanical properties

INTRODUCTION

Continuous fiber ceramic composites (CFCCs) materials are potentially attractive as high-temperature structural materials because of their high-temperature mechanical properties [1]. Damage tolerant characteristics of CFCCs arise because of stress redistribution mechanism, involving matrix cracking and stochastic fiber failure, accompanied by debonding and sliding interface [2]-[7]. Most CFCCs are based on SiC fibers, with either oxide or non-oxide matrices, and with interphases consisting of various combinations of carbon, BN, and SiC. The presence of cracks after processing are rationalized by assessing the coefficient thermal expansion ratio (CTE) and the thermal residual stress [8]. These materials are susceptible to embrittle by oxygen ingress through the matrix cracks [9], [10], which is activated at intermediate temperature (773 K-1173 K) [10]. The embrittlement

problem imposes major design limitations by requiring that the stress remain below the matrix cracking stress [10]. Therefore, control of the residual stress in the composites is required in order to prevent matrix cracking.

Mullite ($3Al_2O_3 . 2SiO_2$) matrix composites are appreciate for use in high-temperature environment [11]. Nakae H. et al. found the formation of primary mullite from a hypereutectic SiO_2-mullite melt [12]. It will be possible that CTE of SiO_2-mullite material is controllable larger or smaller than that of SiC reinforcement ($4.5.10^{-6}$/ K) by controlling volume fraction of primary mullite. Glassy phase in SiO_2-mullite materials will lead to reduction of magnitude of thermal residual stress because of its viscosity, furthermore, will enhance thermal shock resistance of composites because of its low elastic modulus. A sintered SiC fiber with high-temperature phase stability was selected as reinforcement [13].

In order to control the nature of residual stress in the composites, the matrix of three levels of Al_2O_3 content in SiO_2- mullite were prepared. The influence of thermal residual stress on mechanical properties was then investigated.

EXPERIMENTAL PROCEDURE

Three matrix compositions of SiO_2-3.7, 30, 50 mol.%Al_2O_3 were selected in SiO_2-mullite hypereutectic system shown in Fig. 1 [14]. The system has a eutectic point at 1860 K, 3.7 mol.%Al_2O_3. A sintered SiC fiber (Tyranno SA, UBE industry ltd.) with diameters of approximately 8 μm was selected as reinforcement. The fibers were coated with 1μm-thick-layer of carbon by a low-pressure chemical vapor deposition technique (Phyrograph, Toyo Tanso ltd.). This layer has a turbostratic layered structure oriented parallel to the fiber surface.

Eight hundreds tows (1600 filaments/ tow) of carbon-coated Tyranno SA fiber was used. The slurry of each matrix composition was prepared by dispersing the SiO_2 powder (1-FX, 0.1 μm in diameter, Tatsumori ltd.) and Al_2O_3 powder (AKP-30, 0.3 μm in diameter, Sumitomo Chemical ltd.) into distilled water by planetary ball-milling machine. The fiber tows were impregnated by the slurry and then dried at 343 K for 86.4 ks. Green bodies were hot-pressed at the conditions of 30 MPa for 3.6 ks at 1923 K in vacuum (10^{-2}Pa) and then cooled at a rate of 5 K / min.

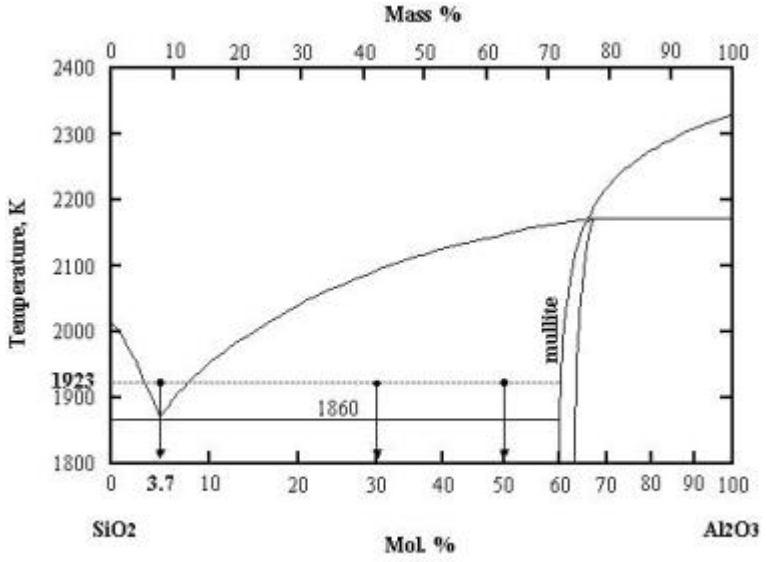

Fig. 1 Phase diagram of SiO2- Al2O3 system.

The density of the each composite was measured by the Archimedes' principle. The microstructure of the composite and the volume fraction of the fibers were examined by optical microscopy. In order to observe morphology of the primary mullite in the matrix, scanning electron microscopy (SEM) observation was carried out. Before SEM observation, composites were polished in transverse section and etched by 48 mass% HF aqueous for 60 sec.

FEM was carried out to calculate thermal residual stress in the composites. 2D typical finite element mesh and boundary conditions are shown in Fig. 2. The symbols of "σ_c", "σ_l" are the maximum principal residual stress of circumferential and longitudinal direction in matrix region respectively. "σ_f" is the stress of radial direction in fiber region. If σ_f is negative, it indicates that fiber is cramped by the matrix. The calculate conditions of FEM are shown in Table 1. Elastic modulus and CTE of the matrices were estimated by using the properties of SiO_2 [15] and mullite [16] by rule of mixture. CTE of mullite ($6.46.10^{-6}$/ K) was measured by thermo-mechanical-analyzer (TMA8310, Rigaku ltd.) for this study individually.

Fiber push-out test was carried out to measure the shear stress at fiber/ matrix interface. A thin slice (130 μm thickness) was cut perpendicular to the fiber axis and polished to about 130 μm thickness. This thin slice was then placed on a resilient substrate with a slit (approximately 300 μm width), and the filaments were individually loaded by the Vickers indenter (MZT-4, Akashi ltd.) until the first evidence of filament movement was found. The first evidence of filament motion was detected by load-constant part in the load vs. displacement curve. The curve generated by measuring the load by a load-cell when pushing on the filament at a constant loading rate of 10 mN/ s up to 150 mN. The interfacial shear stress (τ) was given by the following equation.

$$\tau = F / \pi\, dt$$

where F is the load at which a filament pushed out, d is the filament diameter, and t is the thickness of the specimen.

Three-point flexural tests were conducted on specimens having typical dimensions of 40 mm length, 4 mm width, and 3 mm thickness at a crosshead speed of 0.5 mm/ min and the span of lower pins was 30 mm [17]. Fracture surface was observed by SEM. To examine the contribution of carbon coating to the composites, as-received Tyranno SA fiber reinforced SiO_2-3.7 mol.%Al_2O_3 composite was also fabricated. The absorbed fracture energy was measured by the quasi-static fracture test of three-point flexural specimen with Chevron-notch at a crosshead speed of 0.01 mm/ min and the span of lower pins was 30 mm [18]. The specimens have typical dimensions of 40 mm length, 3 mm width, and 4 mm thickness. A notch with 300 μm width was made in the plane normal to the filament (Fig. 8).

Table 1 The calculate condition of FEM.

	Fiber	Matrix		
		3.7 mol.	30 mol.	50 mol.
Poison's ratio	0.24	0.17	0.3	0.3
Elastic modulus (GPa)	404	70	138	178
CTE (1×10^{-6}/ K)	4.5	0.55	3.74	5.63
Vf (%)	60			
ΔT (K)	1078			

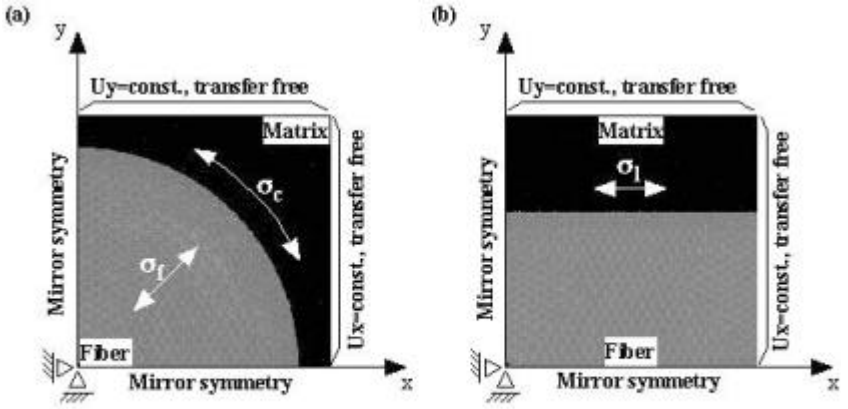

Fig. 6 Typical finite-element mesh (a) transverse section, (b) longitudinal section.

RESULTS AND DISCUSSION

The density and the fiber volume fraction of each obtained composite were approximately 2.5 g/ cm^3 and 70 %, respectively (shown in Table 2). Optical micrographs of a composite are shown in Fig. 3. Matrix cracking due to fabrication process was not observed in each composite.

Table 2 Density and fiber volume fraction of the composites.

Al_2O_3 contect in matrix (mol.%)	3.7	30	50
Density (g/m^3)	2.48	2.63	2.49
Vf (%)	75	73	63

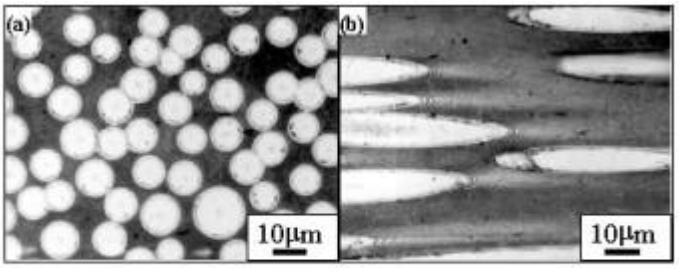

Fig. 3 Optical micrographs of SiCf/ 1μC/ SiO_2- 3.7mol.%Al_2O_3 composites. (a) transverse section, (b) longitudinal section.

SEM images of the composites polished and etched by HF aqueous are shown in Fig. 4. Glassy SiO_2 phase was removed by etching. No chemical reaction between carbon-coating-layer and matrix was found. The matrix of each obtained composite was composed of primary mullite and glass, which means that matrix materials solidified in meta-stable state. In SiO_2-3.7 mol.%Al_2O_3 composite, the morphology of primary mullite shows a kind of faceted whisker. This is because that primary crystal precipitates in preferred growth direction under highly super cooled conditions [11]. The shape of the primary mullite depends on the composition, however, the mullite uniformly distributes in the glassy phase.

The thermal residual stress due to the mismatch of CTE between the fiber and matrix will be induced under the softening point of the glassy phase, which is assumed at 1373 K. FEM was used for calculating the stress at room temperature. The results shown in Table 3 reveal that the nature and magnitude of the stress depends on the Al_2O_3 content in the matrices, which will be caused by increasing in CTE of the matrices with an increase in the Al_2O_3 content.

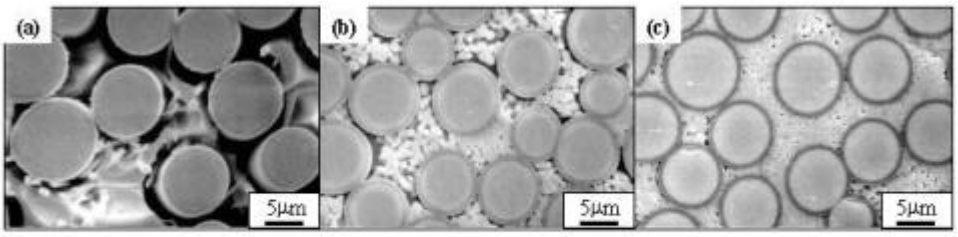

Fig. 4 SEM images of SiCf/ 1μmC/ SiO_2- Mullite composites etched by HF aqueous. (a) 3.7mol. %, (b) 30mol.%, (c) 50mol.% Al_2O_3

Table 3 Calculated residual stress in the composites.

Al_2O_3 content in matrix (mol. %)	Residual stress (GPa)		
	σ_c	σ_l	σ_f
3.7	- 0.34	- 0.27	+ 0.23
30	- 0.12	- 0.09	+ 0.08
50	+ 0.67	+ 0.48	- 0.13

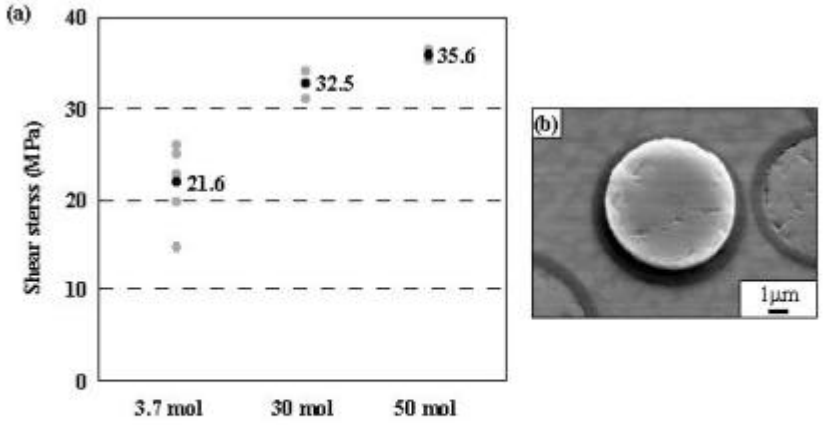

Fig. 5 (a) Interfacial shear stress of SiCf/ 1μmC/ SiO_2- Mullite composites and (b) SEM image of pushed out filament (SiCf/ 1μm/ SiO_2- 30mol.% Al_2O_3 composite).

Fiber/ matrix interfacial shear stress for the composites is shown in Fig. 5 (a). The stress increased with an increase in the Al_2O_3 content in the matrices. It is known that interfacial shear stress is influenced by the debonding shear stress and interfacial frictional stress [19]. Interfacial frictional stress is the function of the residual stress and interfacial roughness. As shown in Fig. 5 (b), the debonding is found at carbon/ SiC interface regardless of the composition of the matrices. Thus, the debonding shear stress and the roughness must be constant independent of the Al_2O_3 content in the matrices. Therefore, residual stress will control the interfacial shear stress. In the transverse section, the nature of fiber-cramping

residual stresses, σf in 3.7, 30 mol. % Al_2O_3 composites tend to promote the debonding of fiber/ matrix interface. Such a debonding due to thermal residual stress was reported by Bischoff E. et al. [20]. On the other hand, the nature of fiber-cramping residual stress in the 50mol. % Al_2O_3 composites prevents interface from debonding.

The flexural strength of the composites is shown in Fig. 6. Fracture surface of a composite after flexural test is shown in Fig. 7. The non-catastrophic failure with fiber pull-out and bridging was found in fracture surfaces of carbon coated fiber reinforced composites regardless of matrix composition. The flexural strength decreases with an increase in the Al_2O_3 content in the matrices. In the longitudinal section, initiation of matrix crack will be suppressed because of compressive residual stress, σl in the matrices as shown in Table 3. Thus, the highest flexural strength of the SiO_2-3.7 mol.% Al_2O_3 matrix composite will be caused by the highest compressive residual stress in the matrix. Average flexural strength of non-coated fiber reinforced SiO_2-3.7 mol%Al_2O_3 composite was 288 MPa with catastrophic fracture. This reveals that the carbon-coating layer is effective to induce the non-catastrophic fracture of as reported in previous works.

Load vs. displacement curves of quasi-static fracture tests are shown in Fig. 8. In all specimens of each composite reinforced by carbon-coated fiber, the stable crack growth was observed with displacement of over 4 mm. The larger strength at which matrix crack initiates from the notch will be caused by larger compressive residual stress in the matrices, similar to the flexural strength of the composites.

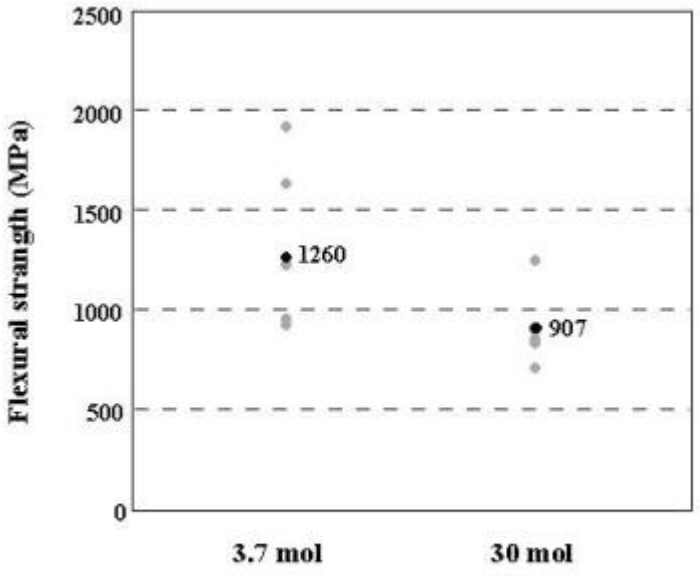

Fig. 6 Flexural strength of SiCf/ 1μmC/ SiO_2- Mullite composites.

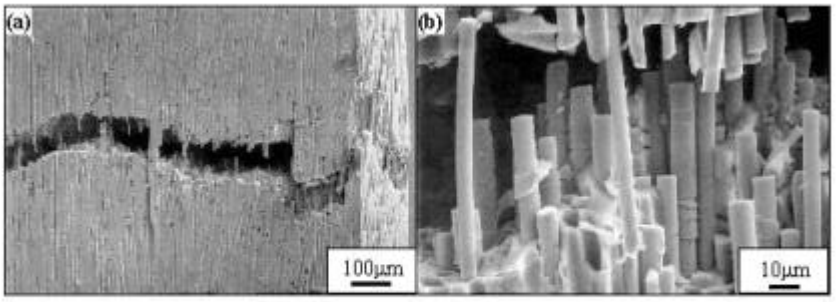

Fig. 7 Fractographs of SiCf/ 1mC/ SiO2-3.67 mol.%Al2O3 composites. (a) low mag., (b) high mag.

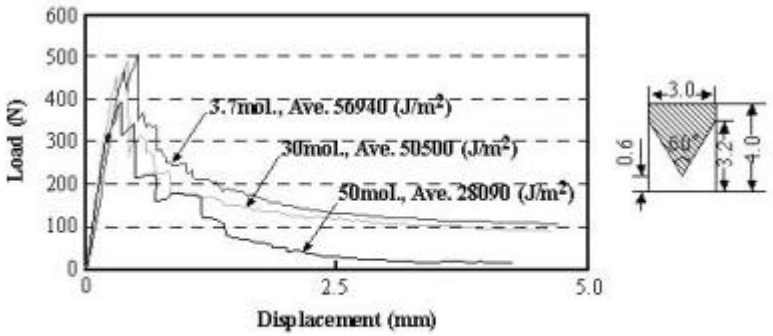

Fig. 8 Load vs. displacement curves of the composites, dimensions of Chevron- notch.

CONCLUSIONS

A sintered SiC fiber reinforced SiO_2-mullite composites were fabricated by impregnation of fiber tows into matrices slurry and hot-pressing. In order to control the nature of residual stress in the composites, the matrix of three levels of Al_2O_3 content in SiO_2- mullite were prepared. Influences of thermal residual stress state to mechanical properties of composites were examined. The results are as follows.

1. No chemical reaction between carbon coating layer and matrix interface was found.
2. The nature of thermal residual stress in the composites are controlled by the Al_2O_3 content in SiO_2-mullite hypereutectic oxide.
3. The highest flexural strength of the SiO_2-3.7 mol.% Al_2O_3 matrix composite will be caused by the highest compressive residual stress in the matrix.

ACKNOWLEDGEMENTS

This work was technically supported by UBE industries, ltd. and Toyo Tanso co., ltd.. We wish to express our appreciation for this support.

REFERENCES

1. Kim H. E. et al., "Oxidation behavior and effects of oxidation on the strength of SiC-whisker reinforced alumina", *J. Mat. Sci.*, 1994, Vol. 29, pp.1656-1661

2. Evans A. G., "Perspective on the development of High- toughness ceramics", *J. Am. Ceram. Soc.*, 1990, Vol. 73, No. 2, pp.187-206
3. Sheldon B. W. et al., "Oxidation of BN-coated SiC fibers in ceramic matrix composites", *J. Am. Ceram. Soc.*, 1996, Vol. 79 No.2, pp.539-543
4. Chyung K. et al., "Fluoromica coated nicalon fiber reinforced glass-ceramics composites", *Material Science and Engineering*, 1993, Vol. A162, pp.27-33
5. Qi G. et al., "Carbon-layer formation at silicon-carbide-glass interfaces", *Material Science and Engineering*, 1993, Vol. A162, pp.45-52
6. Cao H. C. et al., "Effect of interfaces on the properties of fiber-reinforced ceramics", *J. Am. Ceram. Soc.*, 1990, Vol. 73, No. 6, pp.1691-1699
7. Yoshida M. et al., "Fabrication and mechanical properties of SiC fiber reinforced oxide matrix composites", *Proc. of second international conference on processing materials for properties, TMS and The Mining & Materials*, California, 2000, pp.121-126
8. Heredia F. E. et al., "Tensile and shear properties of continuous fiber-reinforced SiC/Al_2O_3 composites processed by melt oxidation", *J. Am. Ceram. Soc.*, 1995, Vol. 78, No. 10, pp.2790-2800
9.Ogasawara T. et al., "Creep behavior of 3D woven Tyranno fiber/Si-Ti-C-O matrix composite", *Report of RIAM symposium No.11 ME-S1, Mechanical behavior of fiber reinforced composites*, 2000, pp.35-38
10. Levi C. G. et al., "Processing and performance of an all-oxide ceramic composite", *J. Am. Ceram. Soc.*, 1998, Vol. 81, No. 8, pp.2077-2086
11. Tsai C. Y. et al., "Effect of zirconia content on the oxidation of silicon carbide/zirconia/mullite composites", *J. Am. Ceram. Soc.*, 1998, Vol. 81, No. 9, pp.2413-2420
12. Nakae H. et al., "Influence of melting temperature on morphology of primary mullite in SiO_2-Al_2O_3 system", *Materials Transactions, JIM*, 1995, Vol. 36 No. 9, pp.1163-1169
13. Ishikawa T. et al., "High-strength alkali-resistant sintered SiC fibre stable to 2, 200.", *Nature*, 1998. Vol. 391, pp.773-775
14. Klug F. J. et al., *J. Am. Ceram. Soc.*, 1987, Vol. 70, No. 10, pp.750-759
15. *JSME mechanical engineers' handbook*, 1984. pp.B4-158
16. *New Ceramics*, 1989, Vol. 5, pp.79-83
17. "Testing method for flexural strength (modulus of rupture) of high performance ceramics", *JIS standards*, 1981, JIS R1601
18. "Testing method for fracture energy of ceramic composites by quasi-static fracture of 3-point bend specimen with Chevron-notch", *Standard of The Ceramic Society of Japan*, 1994, JCRS 201
19. Singh R. N. et al., "Influence of residual stress, interface roughness, and fiber coating on interfacial properties in ceramics composites", *J. Am. Ceram. Soc.*, 1996, Vol. 79, No. 1, pp.137-147
20. Bischoff E. et al., "Microstructural studies of the interfacial zone of a SiC-fiber-reinforced lithium aluminum silicate glass- ceramics, *J. Am. Ceram. Soc.*, 1989, Vol. 72, No. 5, pp.741-745